



Vapor intrusion attenuation factors relative to subslab and source, reconsidered in light of background data

Yijun Yao^{a,b,c,*}, Yun Wu^{a,b,c}, Eric M. Suuberg^d, Jeroen Provoost^e, Rui shen^f,
Jianqing Ma^{a,b,c}, Jing Liu^{a,b,c}

^a MOE Key Lab of Environmental Remediation and Ecosystem Health, College of Environmental and Resource Sciences, Zhejiang University, Hangzhou 310058, China

^b Research Center for Air Pollution and Health, Zhejiang University, Hangzhou 310058, China

^c Institute of Environmental Science, Zhejiang University, Hangzhou 310058, China

^d School of Engineering, Brown University, RI 02912, USA

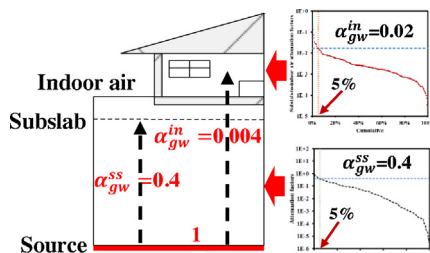
^e Independent Researcher, Espoo, Finland

^f Halliburton Energy Services, Inc., Houston, TX 77032, USA

HIGHLIGHTS

- The influence of VI is determinant if subslab concentration (SC) > 500 $\mu\text{g}/\text{m}^3$.
- When SC < 500 $\mu\text{g}/\text{m}^3$, indoor air concentration is more likely background.
- 0.02 is the generic subslab-to-indoor air concentration attenuation factor.
- 0.004 is the generic groundwater-to-indoor air concentration attenuation factor.

GRAPHICAL ABSTRACT



ARTICLE INFO

Article history:

Received 29 July 2014

Received in revised form 1 January 2015

Accepted 4 January 2015

Available online 7 January 2015

Keywords:

Vapor intrusion

Attenuation factors

Background concentration

Subslab concentration

EPA database

ABSTRACT

The basis upon which recommended attenuation factors for vapor intrusion (VI) have been derived are reconsidered. By making a fitting curve to the plot showing the dependence of observed indoor air concentration (c_{in}) on subslab concentration (c_{ss}) for residences in EPA database, an analytical equation is obtained to identify the relationship among c_{in} , c_{ss} and the averaged background level. The new relationship indicates that subslab measurements may serve as a useful guide only if c_{ss} is above 500 $\mu\text{g}/\text{m}^3$. Otherwise, c_{in} is independent of c_{ss} , with a distribution in good agreements with other studies of background levels. Therefore, employing this screening value (500 $\mu\text{g}/\text{m}^3$), new contaminant concentration attenuation factors are proposed for VI, and the values for groundwater-to-indoor and subslab-to-indoor air concentration attenuation factors are 0.004 and 0.02, respectively. The former is applied to examining the reported temporal variations of c_{in} obtained during a long-term monitoring study. The results show that using this new groundwater-to-indoor air concentration attenuation factor also provides a reasonably conservative estimate of c_{in} .

© 2015 Elsevier B.V. All rights reserved.

1. Introduction

The U.S. EPA has recommended the use of empirical attenuation factors during preliminary vapor intrusion (VI) screening [1]. These factors permit estimation of contaminant indoor air concentrations (c_{in}) in a structure of concern, by relating these

* Corresponding author at: MOE Key Lab of Environmental Remediation and Ecosystem Health, College of Environmental and Resource Sciences, Zhejiang University, Hangzhou 310058, China. Tel.: +86 571 8898 2470.

E-mail address: Yijun.Yao@zju.edu.cn (Y. Yao).

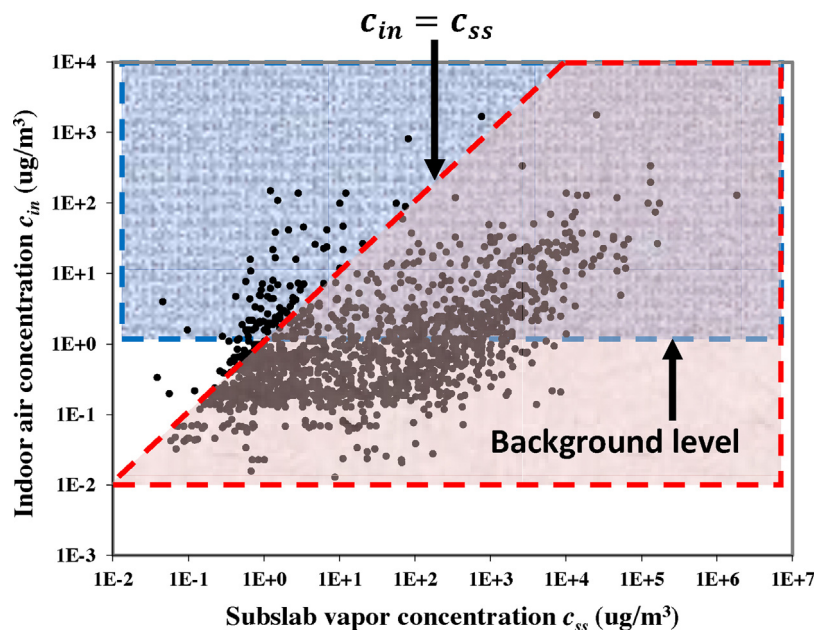


Fig. 1. The selected subsets in EPA's VI database used to calculate generic attenuation factors [1,3]. (For interpretation of the references to color in text, the reader is referred to the web version of this article.)

to corresponding subsurface contaminant vapor concentrations, through use of empirically obtained ratios ($\alpha = c_{in}/c_{subsurface}$). Typically, the selected subsurface soil gas concentration is that beneath the slab on which a structure of interest sits. If available, this subsurface concentration is the so-called subslab concentration (c_{ss}) measured directly beneath the building's foundation slab. Since this value is generally not available during a preliminary screening, the reference subsurface concentration is then the contaminant vapor concentration in equilibrium with a groundwater contaminant source located beneath the structure (c_{gw}). This presumes the usual VI scenario of contaminated groundwater serving as the source of contaminant vapor.

These attenuation factors can be estimated from mathematic models (i.e., the Johnson–Ettinger (J–E) model [2] or from the cases recorded in the U.S. EPA's VI database of field measurements [3]). The J–E model has been implemented as a widely-used screening tool, from which estimates of attenuation factors are readily available [4]. Recently, Johnston and Gibson have extended this underlying modeling tool using a more probabilistic than deterministic approach [5], and also suggested updating key input parameters for that model with Bayesian calibration [6], which method was also used in other modelling studies [7–9]. However, the use of VI models still requires many inputs involving the features of soil and building construction and operation, which sometimes are difficult to characterize [6]. Besides, there are with certain modeling approaches inherent physical restrictions that may or may not reflect the actual situation, such as the imposition of a particular form of mass conservation inherent in most one-dimensional screening tools, including the J–E approach [10]. The consequence of this is not necessarily physically realistic, such as when all subsurface contaminant is forced to flow through a structure [11].

Compared to VI models, the use of generic attenuation factors can provide a conservative estimate of c_{in} more easily, without the difficulties inherent in the above approaches. However, this is an empirical approach and in developing it for certain situations, attention must be paid to certain aspects that an empirical approach cannot properly capture. A major concern is that the subject of this paper is associated with the influence of background sources, which refer to both indoor and outdoor non-VI sources

that can affect indoor air quality, in the VI database on which these empirical values are based [12,13]. Though the threshold background levels were provided for individual chemicals based on other studies, there were no actual measurements for the background concentration for the subsets recorded in this database. To minimize the influences of background sources, two different sets of criteria were applied by the U.S. EPA in the development of the generic attenuation factors. The U.S. EPA's draft guidance [1] shows the groundwater-to-indoor air attenuation factor is ($\alpha_{gw}^{in} = c_{in}/c_{gw}$) for 95% of structures exhibiting c_{in} at above typical background levels; this portion of the data is shown as the shaded blue rectangle in Fig. 1. Note that while the discussion here is about α_{gw}^{in} , the data of Fig. 1 are themselves plotted as a function of measured c_{ss} , as this will be the main focus of the later discussion.

It must also be noted that Fig. 1 includes data for a variety of contaminants of concern. The background levels of these different contaminants of concern are all actually different, but close enough on the chosen logarithmic scale as to be indistinguishable. A statistical analysis of factors influencing attenuation factors also showed that the influences of differing molecular weights and diffusivities of contaminants are small [14]. So for the moment they are treated as the same (distinctions between different contaminants will be shown below).

The red-shaded trapezoidal area of Fig. 1 shows the area of data points for which measured c_{ss} exceeds c_{in} , as would be expected in scenarios in which VI might control c_{in} . U.S. EPA's draft guidance reported that shallow soil gas-to-indoor air attenuation factors were less than 0.1 for 85% of the residences in 2002. It should be noted that the soil gas samples obtained 5 feet below foundation level and c_{ss} was treated as shallow soil gas samples in the initial analysis [1]. Theoretically, shallow soil gas concentration should be higher than c_{ss} , which means the “true” value of the generic $\alpha_{ss}^{in} = c_{in}/c_{ss}$ should also be higher than 0.1. However, many of the points in this dataset are problematic, because they fall below the line associated with non-VI background concentrations; this will be the subject of further discussion below. Based on the analysis of the data sets available in 2002, 0.001 and 0.1 were recommended by the U.S. EPA as the generic α_{gw}^{in} and α_{ss}^{in} , respectively [1]. In a more recent EPA report, these values were corrected

to 0.001 and 0.03, respectively, by applying source strength screens to an updated VI database [15]. In this paper, we will re-examine these values ($\alpha_{ss}^{in} = 0.1$ and $\alpha_{gw}^{in} = 0.001$ recommended by EPA in 2002; $\alpha_{ss}^{in} = 0.03$ and $\alpha_{gw}^{in} = 0.001$ recommended by EPA in 2012) in the context of both physical models of the processes, as well as consideration of background concentrations.

It is critical to consider the influences of background sources in the process of obtaining both of these attenuation factor values [1]. For example, c_{in} appears to be relatively independent of c_{ss} when the latter is relatively low, because non-VI background sources are more important in determining c_{in} under these conditions [15,16]. Two EPA reports have in fact suggested that it might be appropriate to use the c_{ss} to determine whether c_{in} is influenced by background sources [12,15]. Another report has offered a way of calculationally reconciling the empirical attenuation factors from the field data with “true” attenuation factors [15]. In this study, we re-examine the issue of empirical attenuation factors for non-biodegradable contaminants focusing on structures with high c_{ss} such that c_{in} can unambiguously be linked to subsurface contaminant vapor sources.

2. The physical basis of attenuation factors

2.1. Contaminant vapor concentration profiles in soil and attenuation factors

The general governing equation for soil vapor transport is [17]:

$$\phi_{g,w,s} \frac{\partial c_{ig}}{\partial t} = -\nabla \times (q_g c_{ig}) - \nabla \times \left(\frac{c_{ig}}{H_i} q_w \right) + \nabla \times (D_i \nabla c_{ig}) - R_i \quad (1)$$

$$\text{where } \phi_{g,w,s} = \phi_g + \frac{\phi_w}{H_i} + \frac{k_{oc,i} f_{oc} \rho_b}{H_i} \quad (2)$$

In Eqs. (1) and (2), $\phi_{g,w,s} \partial c_{ig} / \partial t$ represents transient term of contaminant transport in three phases: gas, soil and moisture; $-\nabla \times (q_g c_{ig}) - \nabla \times \left(\frac{c_{ig}}{H_i} q_w \right)$ refers to the convection term driven by soil gas or groundwater flow; $\nabla \times (D_i \nabla c_{ig})$ describes the diffusion of contaminant soil gas; q_g is the soil gas flow per unit area [$L^3_{gas}/L^2_{soil}/T$]; q_w is the groundwater flow per unit area [$L^3_{water}/L^2_{soil}/T$]; ϕ_g is the air filled porosity [L^3_{gas}/L^3_{soil}]; ϕ_w is the moisture filled porosity [L^3_{water}/L^3_{soil}]; H_i is the contaminant Henry's Law constant [$(M_i/L^3_{gas})/(M_i/L^3_{water})$], linearly relating vapor phase contaminant concentration to water phase concentration; $k_{oc,i}$ is the sorption coefficient of contaminant i to organic carbon in the soil [$(M_i/M_{oc})/(M_i/L^3_{water})$]; f_{oc} is the mass fraction of organic carbon in the soil [M_{oc}/M_{soil}]; ρ_b is the soil bulk density [M_{soil}/L^3_{soil}]; c_{ig} is the concentration of contaminant i in the gas phase [M_i/L^3_{gas}]; D_i is overall effective diffusion coefficient for transport of contaminant i in porous media [L^2/T]; R_i is the contaminant i loss rate by biodegradation [$M_i/L^3_{soil}/T$] and $\phi_{g,w,s}$ is the effective transport porosity [L^3_{air}/L^3_{soil}], defined in Eq. (2).

In most studies, the steady state cases receive most attention, for which $\phi_{g,w,s} \partial c_{ig} / \partial t = 0$. Then, Eq. (1) becomes:

$$0 = -\nabla \times (q_g c_{ig}) - \nabla \times \left(\frac{c_{ig}}{H_i} q_w \right) + \nabla \times (D_i \nabla c_{ig}) - R_i \quad (3)$$

Previous studies have shown that the convection induced by indoor air-atmosphere pressure differences affect contaminant concentration distributions only around the immediate vicinity of a foundation crack, through which the pressure difference is communicated into the soil [17,18]. The general soil gas contaminant concentration profile is then determined mainly by diffusive transport through the soil. Thus, throughout most of the soil domain surrounding the structure of interest, the convection term is negligible [19], and

$$0 = \nabla \times (D_i \nabla c_{ig}) - R_i \quad (4)$$

There are two major classes of contaminants of concern for VI in U.S.—the chlorinated solvents, including tetrachloroethylene (PCE) and trichloroethylene (TCE), and the other includes petroleum hydrocarbons. In China, the major contaminants includes pesticide [20–23]. The former class is predominant in the U.S. EPA's VI database. This class is usually considered as non-biodegradable, so the assumption of $R_i = 0$ can be applied in that case. Assuming further that the contaminant diffusivity in soil gas is not position dependent,

$$D_i \nabla^2 c_{ig} = D_i \nabla^2 \frac{c_{ig}}{c_{is}} = 0 \quad (5)$$

where c_{is} , the contaminant i source vapor concentration [M_i/L^3_{gas}], has been introduced as a constant that non-dimensionalizes the concentration profile that is obtained from Eq. (5). By virtue of the fact that the diffusivity D_i has been assumed constant, it is immediately apparent that its value can be dropped from Eq. (5), and that the solution of the concentration profile from Eq. (5) will not depend upon this value (for the usual assumptions of fixed vapor source and atmospheric concentrations of contaminant).

The non-dimensional soil gas concentration profile (c_{ig}/c_{is}) in any layer of constant diffusivity is thus independent of c_{is} , but the profiles in actual complex soils with non-constant diffusivity will be determined by the distribution of D_i . Other factors influencing the profile include the geometry and dimensions of the model domain and its associated boundary conditions. In a typical VI scenario, involving a building surrounded by open ground surface and with a uniform contaminant vapor source beneath the building, the non-dimensional contaminant subsurface concentration (c_{ss}/c_{gw}) is affected by soil properties, including the distribution of effective diffusivity, and boundary conditions. It is the solution of Eq. (5) in three coordinate directions, with imposition of what is largely a no-flux boundary condition defined by the building's slab, that results in a contaminant concentration profile which typically gives highest values directly beneath the slab [24].

Thus, in the soil domain between contaminant vapor source and subsurface, it is Eq. (5) that must determine the attenuation factor. No one-dimensional analysis of the diffusion process beneath a building can offer a completely reliable estimate of this attenuation factor, because the inherently three-dimensional nature of the real soil gas diffusion process requires accounting for lateral diffusion, as well as vertical, though in certain situations the one-dimensional approximation may be adequate [10,17]. The key points to emphasize are that source-to-subsurface attenuation factors cannot be expected to depend upon contaminant diffusivity, if an assumption of uniform soil properties is employed; the profile will be purely geometrically determined. If non-uniform soil diffusivity is involved, then the details of how diffusivity varies with position become important (and Eq. (4), rather than Eq. (5), determines the source-to-subsurface attenuation factor).

2.2. The attenuation of contaminant vapor concentration during entry into a building

The attenuation from subsurface to indoor air can be expressed as [2]:

$$\frac{c_{in}}{c_{ss}} \approx \begin{cases} \frac{Q_s}{V_b A_e} \\ 1 - \exp\left(-\frac{Q_s d_{ck}}{A_{ck} D_{ck}}\right) \\ \frac{A_{ck} D_{ck}}{d_{ck} V_b A_e}, \end{cases} \quad \begin{matrix} Q_s \neq 0 \\ \\ Q_s = 0 \end{matrix} \quad (6)$$

where V_b is the enclosed space volume [L^3], and A_e is the indoor air exchange rate due to ventilation [$1/T$]; Q_s is the volumetric flow rate of soil gas into the enclosed space [L^3/T], A_{ck} is the area of the

crack [L^2], D_{ck} is the contaminant effective diffusivity in the crack [L^2/T] and d_{ck} is the thickness of the crack [L]. $c_{in} \ll c_{ss}$ is assumed, consistent with a significant subslab to indoor air attenuation of contaminant concentration. Often, the Nazaroff equation has been used to provide an estimate of soil gas entry rate into a building, subject to a perimeter crack assumption [2,25].

$$Q_s = \frac{2\pi k \Delta p L_{ck}}{\mu_g \ln(2d_f/w_{ck})} \quad (7)$$

in which μ_g is the soil gas viscosity [$M/L/T$], L_{ck} is the total length of perimeter crack [L], w_{ck} is its width [L], k is the soil permeability [L^2], d_f is the depth at which the crack is located, and Δp is the indoor depressurization driving force [$M/L/T^2$].

Johnston and Gibson [14] reported that the soil type plays a significant role in influencing attenuation factor, with fine-grained soils giving lower values than coarse-grained. This is understood in terms of the influence of permeability on the soil gas entry rate, as illustrated in Eq. (9). Also, the attenuation factors are higher in winter, in which stack effect depressurization (Δp) is expected to be high and air exchange rate lower, except for crawl-space houses [14]. Consequently, the attenuation factors for soil transport (and the source-to-subslab attenuation) and for building entry (and the α_{ss}^{in}) are governed by different physical variables, and there is no reason to expect that the values of these attenuation factors should be related to each other.

3. EPA's VI database and screening methods

The U.S. EPA's VI database is a collection of measured data from VI sites throughout U.S. [3]. The database contains information from 43 sites and 21 kinds of chemicals, such as chlorinated chemicals and BTEX. But the focus is the former. 2458 total residence and chemical combinations are included in this database. In general, the EPA database contain enough representative records to generate empirical conservative attenuation factors.

However, before the information in the database can be used to calculate the "true" α_{gw}^{in} and α_{ss}^{in} , the influences of background sources should be minimized by screening in subsets with c_{in} most likely determined by subsurface sources. In EPA's 2012 report, source strength screens were employed [15]. The key of this technique is to exclude subsets with low subsurface soil gas concentration, based on an assumption that c_{in} in subsets with large attenuations factors from subsurface to indoor air are more likely to be influenced by background sources.

In this study, a fitting curve is made for the plot showing the dependence of c_{in} on c_{ss} , providing an analytical relationship among c_{in} , c_{ss} and background levels, based on all calculated α_{ss}^{in} recorded in the database. Based on this equation, a critical c_{ss} can be found as the criterion to determine the possible influence of subsurface sources on indoor air quality. By screening in subsets with higher c_{ss} than this critical value, the distributions of calculated attenuation factors were obtained to develop conservative empirical attenuation factors including both α_{gw}^{in} and α_{ss}^{in} , independent of background levels. For α_{gw}^{ss} employed in this study, such criteria is not applied. For all analysis, the subsets with c_{in} less than the reporting limits were excluded. The generic attenuation factors (α_{gw}^{in} , α_{ss}^{in} and α_{gw}^{ss}) recommended in this study were defined as the values higher than the corresponding attenuation factors for 95% of the screened subsets in EPA database. As recommended by EPA in 2002 and 2012 [1,15], these values could be considered as generally reasonable upper-bound values.

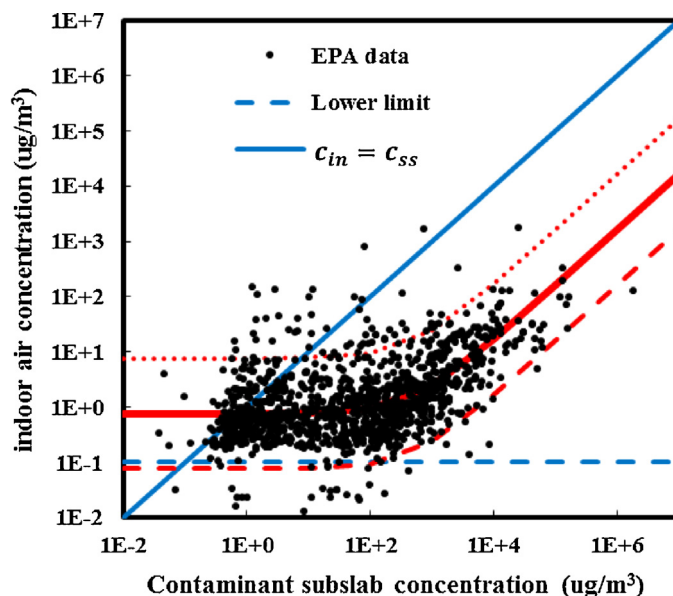


Fig. 2. The influences of measured contaminant subslab concentration (c_{ss}) on measured indoor air concentration (c_{in}) in U.S. EPA's VI Database. (The fitting curve was made based on $\log(c_{in})$ instead of c_{in}) [3]. (For interpretation of the references to color in text, the reader is referred to the web version of this article.)

4. Results and discussion

4.1. Subslab-to-indoor air concentration attenuation factor

Based upon the assumption of crack entry, the soil gas entry rate can be estimated from the Nazaroff equation above. Key to obtaining "good" values of c_{in} is having knowledge of the building ventilation conditions. It can be challenging to obtain such estimates, since often building ventilation is dynamically variable.

Still, it is instructive to calculate estimates of attenuation factor, based upon a "typical" VI scenario [17], where $V_b = 174 \text{ m}^3$, $A_e = 0.5 \text{ h}^{-1}$, $k = 10^{-11} \text{ m}^2$, $\Delta p = -20 \text{ Pa}$, -5 Pa or 0 Pa , $L_{ck} = 39 \text{ m}$, $\mu_g = 0.0648 \text{ kg/m/h}$, $d_f = 2 \text{ m}$, $d_{ck} = 0.15 \text{ m}$, $D_{ck} = 8.8 \times 10^{-6} \text{ m}^2$ and $w_{ck} = 0.001 \text{ m}$. According to Eqs. (6) and (7), we can estimate that

$$\frac{c_{in}}{c_{ss}} = \frac{J_s}{V_b A_e c_{ss}} = \begin{cases} 1.3 \times 10^{-2}, \Delta p = -20 \text{ Pa} \\ 3.4 \times 10^{-3}, \Delta p = -5 \text{ Pa} \\ 9.3 \times 10^{-5}, \Delta p = 0 \text{ Pa} \end{cases} \quad (8)$$

Again, background concentration is not considered in Eq. (8). These results suggest that for "typical" conditions, the attenuation factors for subslab to building interior should be of order 10^{-2} – 10^{-4} , for a typical ventilation rate. Again, if A_e were to approach zero, c_{in} would necessarily approach c_{ss} , and the attenuation factor would approach unity. Fig. 2 shows the influence of observed c_{ss} on observed c_{in} in U.S. EPA's VI database. The subsets with c_{in} less than the reporting limit are excluded and the remaining used in this figure is from 15 VI sites, sampled over a time period from 1995 to 2005 and including 1268 observations. The solid blue line represents where c_{ss} and c_{in} are equal, which is normally not expected for reasons already discussed. Clearly, the majority of c_{ss} are higher than c_{in} , indicating some attenuation. There are sites where c_{ss} is actually lower than the c_{in} which must indicate the existence of other sources (outdoor air, sink, building materials, etc.). There appears to be a lower limit (horizontal dashed blue line) for the observed c_{in} at around $0.1 \text{ } \mu\text{g/m}^3$. This is near typical detection or reporting limits for the compounds of concern [12]. Basically, the figure can be divided into two parts [12]. When c_{ss} is less than $100 \sim 1000 \text{ } \mu\text{g/m}^3$, most of the c_{in} data fall

in the range between 0.1 and $10 \mu\text{g}/\text{m}^3$, with no real dependence on c_{ss} . As discussed elsewhere, such data strongly suggest the role of background concentration [12,15,26]. When c_{ss} is above about $100\text{--}1000 \mu\text{g}/\text{m}^3$, a trend emerges, showing that c_{in} increases with c_{ss} . This indicates that the influence of subsurface sources becomes dominant over background sources [15]. The data in Fig. 2 were subjected to a curve-fitting exercise that reflected this trend. The result may be expressed as:

$$c_{in} \approx 1.6 \times 10^{-3} c_{ss} + 0.8 \mu\text{g}/\text{m}^3 \quad (9)$$

where c_{ss} is the contaminant subslab concentration [$\mu\text{g}/\text{m}^3$], $0.8 \mu\text{g}/\text{m}^3$ is the averaged background concentration (again, independent of contaminant types); and 1.6×10^{-3} thus, represents an average α_{ss}^{in} . The results of the correlation are shown in Fig. 2, as the solid red line. It should be recognized that the curve in Fig. 2 is not linear despite the form of Eq. (11), because Fig. 2 is drawn on logarithmic axes.

Multiplying Eq. (9) by (10) and 0.1 a family of lines is obtained, as also shown in Fig. 2. The choice to vary the correlation by an order of magnitude is arbitrary, but it serves to illustrate that the majority of data in the U.S. EPA database are captured to within an order of magnitude of the correlation Eq. (12).

$$c_{in} = \begin{cases} 1.6 \times 10^{-2} c_{ss} + 8 \mu\text{g}/\text{m}^3, & \text{max(dotted red line in Fig. 2)} \\ 1.6 \times 10^{-3} c_{ss} + 0.8 \mu\text{g}/\text{m}^3, & \text{med(solid red line in Fig. 2)} \\ 1.6 \times 10^{-4} c_{ss} + 0.08 \mu\text{g}/\text{m}^3, & \text{min(dashed red line in Fig. 2)} \end{cases} \quad (10)$$

Eq. (10) shows a similar range of variation in attenuation factors as did Eq. (8), but of course the parameters were selected to show what parameter ranges are needed to see an order of magnitude spread about the mean. More to the point is that the conservative values of predicted and correlated α_{ss}^{in} are actually quite similar. Both values are consistent with the 95th percentile value of 0.03 derived in EPA's 2012 report other than 0.1 in the initial draft guidance [1,15].

Eq. (9) also provides a possibility of determining the influence of subsurface sources on c_{in} . Generally, in Figs. 1 and 2 c_{in} increases with c_{ss} , only if c_{ss} is high. This suggests the dominant role of subsurface sources in those cases, whereas background determines c_{in} in cases with low c_{ss} . There may be a concern that for a few cases with low c_{ss} , the value of c_{in} might still be influenced by VI; for example, a preferential pathway might be involved. Disregarding this possibility for the moment, consider the data for low c_{ss} cases. Fig. 2 shows that the correlation line began bending upward only at c_{ss} of a few $100 \mu\text{g}/\text{m}^3$. Thus, examining data above this range of c_{ss} should allow establishing an attenuation factor for conditions free from background influences.

Fig. 3 shows the distribution of the subset of attenuation factors corresponding to structures in the U.S. EPA's VI database with c_{ss} greater than $500 \mu\text{g}/\text{m}^3$. The value of $500 \mu\text{g}/\text{m}^3$ is obtained by considering where the "knee" of the curve is in Fig. 2, and this corresponds to $(0.8/1.6 \times 10^{-3})$, effectively the absolute value of the x intercept of the correlation line (Eq. (9)) when $c_{in} = 0$. According to Fig. 3, fewer than 5% of these structures show attenuation factors greater than 0.017. This value is consistent with the predictions for the rather conservative 20 Pa depressurization case in Eq. (8).

The results of Fig. 3 are also consistent with the dotted red line of Fig. 2, which is seen to capture most of the data, and which also implies an attenuation factor of around 10^{-2} , as seen from Eq. (10). This is hardly surprising, since both results are obtained from the same underlying data, just analyzed differently. This means that c_{in} is not expected to exceed approximately 0.02 of the measured c_{ss} in 95% of cases, a number that comes from measured field results in which VI is a key determinant of c_{in} . This value is also consistent with the physics of the process, as described by Eq. (8). Consequently, use of an attenuation factor of 0.1 implies a very conservative approach, biased by inclusion of data that are quite likely strongly influenced by background concentrations (see below).

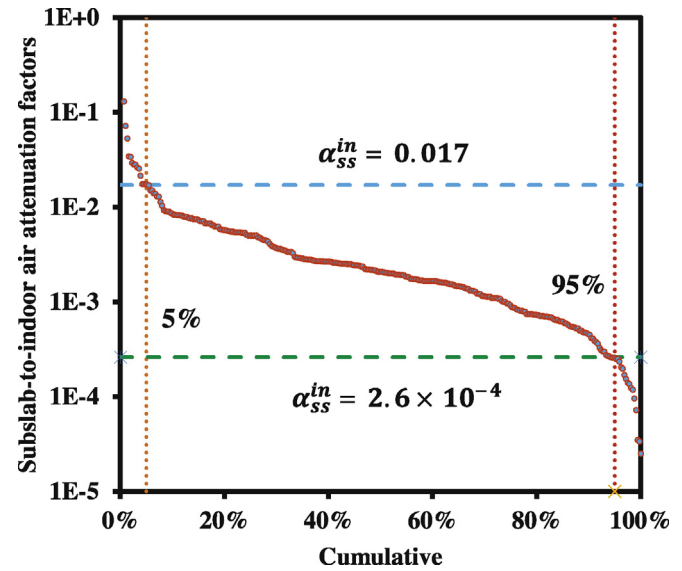


Fig. 3. Distribution of subslab-to-indoor air attenuation factors (α_{ss}^{in}) for all residences in U.S. EPA's VI database with subslab concentration above $500 \mu\text{g}/\text{m}^3$ [3]. (For interpretation of the references to color in text, the reader is referred to the web version of this article.)

The threshold background concentrations recorded in EPA database are different for different contaminants. Regardless of which contaminant is considered, it might be of concern that values approaching $10 \mu\text{g}/\text{m}^3$, as implied by the dotted red curve of Fig. 2, cannot be dismissed as background, and that this could influence the conclusions above regarding values of the attenuation factor in vapor intrusion scenarios. To address these concerns, the data for PCE and TCE were individually considered. Fig. 4a and b was prepared from the U.S. EPA VI database, selecting only those data meeting the criterion of falling below the $500 \mu\text{g}/\text{m}^3$ cutoff. These data are compared with other published data from non-VI indoor air studies [27–31]. The results from Dawson and MacAlary [27] actually summarized some of the other datasets shown, but the individual results are given just to provide a sense that the summary captured well many other study results. Also shown are data from commercial and government buildings [30] that are not strictly comparable to what are otherwise residential studies, but these data again help to establish the spread of data in non-VI influenced structures.

Fig. 4a shows that there is an excellent agreement between the distribution of indoor air PCE concentrations from studies at VI sites (those in the U.S. EPA VI database, for which $c_{ss} < 500 \mu\text{g}/\text{m}^3$), and the results from non-VI sites. The implication is clear, that even when values toward the higher end of c_{in} data distribution are found among the low c_{ss} data, they cannot immediately be ascribed to the effects of VI. Fig. 4b shows the same analysis for TCE, and while the agreement between the two different populations of data is not as impressive as for PCE, the same general conclusion is suggested.

At the very least, these results warn strongly about basing conclusions regarding α_{ss}^{in} on large datasets containing many relatively low c_{ss} values. It would, however, be inappropriate to conclude that when c_{ss} is below the threshold used here ($500 \mu\text{g}/\text{m}^3$), there is no hope of, or need for, proving a completed pathway. Even using the presently suggested most probable α_{ss}^{in} of 0.02 will lead, at the $500 \mu\text{g}/\text{m}^3$ end of the c_{ss} range, to what is generally regarded as unacceptably high c_{in} . Where the present results do point is being more critical when c_{ss} is substantially lower than this.

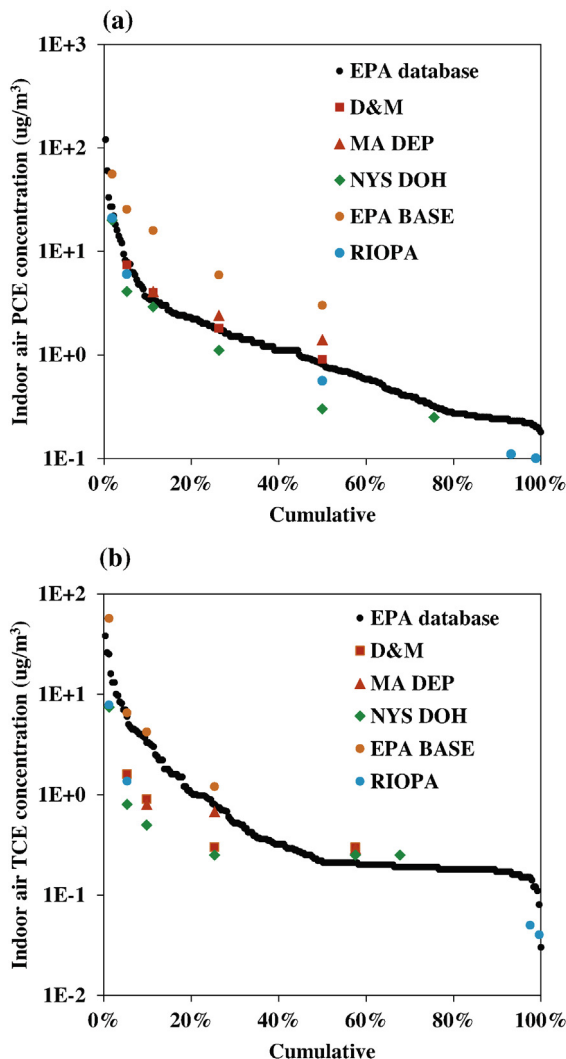


Fig. 4. Comparison between the distribution of indoor air concentration with subslab concentration (c_{ss}) below $500 \mu\text{g}/\text{m}^3$ in the EPA database, with other background studies [3,26–30].

4.2. The groundwater-to-subslab concentration attenuation factor

Fig. 5 shows the distribution of groundwater source-to-subslab attenuation factors ($\alpha_{gw}^{ss} = c_{ss}/c_{gw}$) for all structures in U.S. EPA's VI database, including 282 subsets without applying the screening criteria of $500 \mu\text{g}/\text{m}^3$. Again, c_{gw} is calculated using Henry's law constant based on the measured contaminant concentration in groundwater, and an estimate or measurement of groundwater temperature. Considering all the data, shown as the solid curve, α_{gw}^{ss} range from 10^2 to 10^{-6} . It is clear that any physically reasonable model of steady state VI requires that attenuation factors be 1 or less; values greater than this are possible in certain transient situations, or if there is a strong non-VI indoor source. Fewer than 5% of the structures show attenuation factors greater than 0.6. After eliminating the data with c_{ss} higher than c_{gw} , the dashed curve of Fig. 5 can be constructed. In so doing, fewer than 5% of the structures show source-to-subslab attenuation factors greater than 0.4. Still, a very significant fraction of structures show a source-to-subslab attenuation factor whose value is much higher than the previously recommended α_{gw}^{ss} as 0.01 [1].

As illustrated by Eq. (5), without taking biodegradation into consideration [32,33], a conservative estimate of source-to-subslab attenuation factor could be obtained by assuming that the contaminant source plume is located just beneath the building and is separated from it by uniform soil of constant diffusivity. In such scenarios, the contaminant groundwater source-to-subslab concentration would be determined by the geometry and the boundary conditions, including the building foundation depth (d_f) and source depth (d_s). In Abreu and Johnson's study [17], this scenario was simulated by employing different building foundation type ($d_f = 2$ and 0.2 m for basement and slab-on-grade cases, respectively), source depth ($d_s = 3 \sim 18$ m) and indoor depressurization ($\Delta p = -20 \sim 5$ Pa). Their study indicated that the simulated α_{gw}^{ss} in most cases ranged from 0.1 to 1. This is consistent with Yao et al.'s approximation that used the square root of the ratio of foundation to source depth to predict c_{ss} [19]. Both studies, which used a similar physical modeling framework; were thus, predicting attenuation factors that were at the far upper end of the actually measured values. Clearly, there was a significant additional resistance in the systems that these models were not yet properly capturing.

It must also be recalled that despite the often stated conclusion that some degree of backflow of contaminants into subslab is possible, the contaminant concentration in the subslab zone is still likely to be much less sensitive to building operational parameters than is c_{in} [34]. Thus, it appears unlikely that the six orders of magnitude variation in source-to-subslab attenuation is attributable to temporal effects. Moreover, the effect of building construction differences is not nearly significant enough to induce such variation [14].

In steady state cases (without biodegradation), the observed six orders of magnitude variation of α_{gw}^{ss} might be associated with some variability in soil properties [35]. Recalling the discussion of Eq. (5), it is unlikely that vapor diffusivity in dry soil can be invoked to explain such a large difference. Again, in uniform soil, the contaminant vapor profile does not depend upon soil diffusivity in any case. On the other hand, previous studies [36,37] have shown that the c_{ss} profile is sensitive to the vertical moisture content variation in the soil. This includes a critical role of the capillary fringe above the groundwater, which acts as a very significant vapor diffusion barrier. This resistance has been shown to result in a two order of magnitude decrease in contaminant vapor concentration

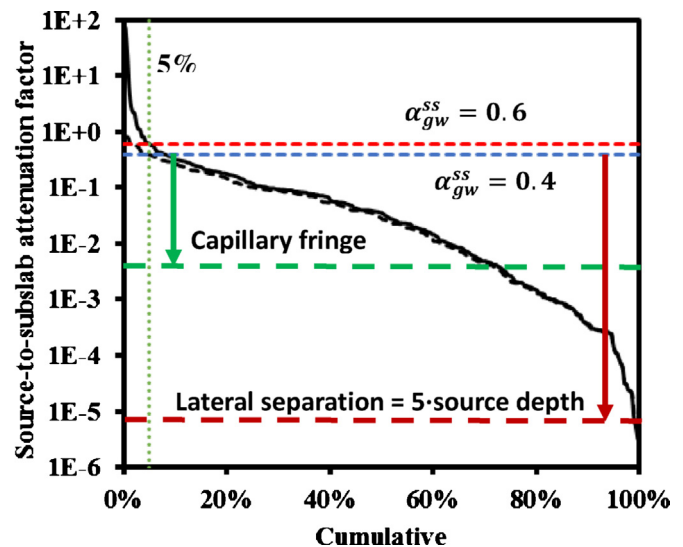


Fig. 5. Distribution of source-to-subslab contaminant attenuation factors for all structures in U.S. EPA's VI database [3,37,39].

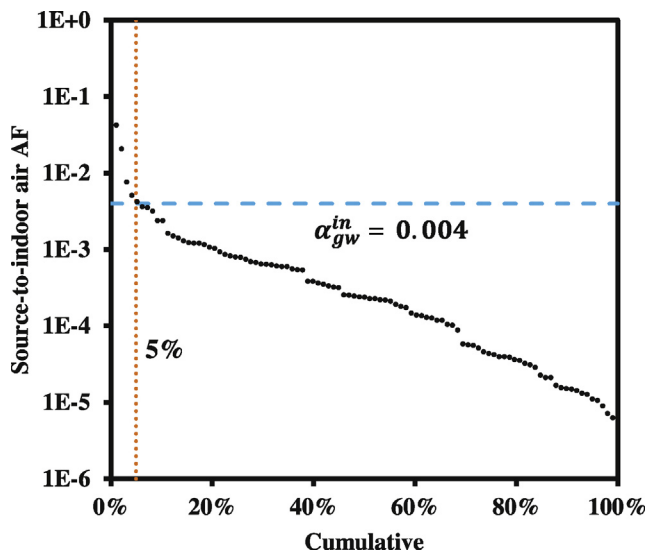


Fig. 6. Distribution of source-to-indoor air AFs for all residences in U.S. EPA's VI database with subslab concentration (c_{ss}) above $500 \mu\text{g}/\text{m}^3$ [3].

immediately above the groundwater source [37]. Thus, if the contaminant vapor source is thought to be the very top of a water table, and there is a relatively clean capillary fringe immediately above this, then using an average partially dried soil diffusion coefficient for this layer will greatly underestimate soil diffusion resistance (and thus, lead to values of soil to subslab attenuation factor that are far too high). The influence of a capillary layer is qualitatively shown in Fig. 5, but it must be understood that there is great complexity associated with modeling this zone. It is critically important to know what the actual vertical concentration profile of contaminant in water is, to do so properly. This shows the inherent weakness of an approach based upon using a groundwater measurement combined with Henry's law, to estimate source strength. More reliable would be use of a soil gas composition measurement from directly above the capillary zone.

Another complication has to do with the lateral separation of a source from a building of concern. Modeling work has shown that there is an exponential decay of soil vapor concentration when moving away from the edge of a contaminated plume [24,38,39]. This fact has been of benefit in defining the maximum distance from plumes to which VI investigations need to be carried out. Conversely, this exponential decay can also confound the results of investigations that involve sampling groundwater too far from a structure of interest. This is particularly the case if a contaminated plume of groundwater exhibits significant lateral concentration gradients. The qualitative influence of a source separated from the footprint of a building of interest by a distance equal to 5 times the depth of the source, is illustrated in Fig. 5 [27].

4.3. The generic groundwater-to-indoor air concentration attenuation factor

Fig. 6 shows the distribution of attenuation factors (α_{gw}^{in}) for structures in U.S. EPA's VI database for which c_{in} and corresponding c_{gw} are available, and for which c_{ss} exceed $500 \mu\text{g}/\text{m}^3$, such that the influences of background concentrations are minimized. Since the number of subsets with c_{gw} , c_{ss} and c_{in} is limited, only 98 observations are found to satisfy the criterion of $c_{ss} > 500 \mu\text{g}/\text{m}^3$ in Fig. 6, where α_{gw}^{in} range from 0.1 to 10^{-6} , with 95% of the data showing values of 0.004 or less. This value is consistent with the maximum α_{ss}^{in} (0.4) from Fig. 5, and the earlier derived α_{ss}^{in} of 0.02. Johnston and Gibson [14] likewise showed that this value (0.004) would be

conservative for most cases in EPA database, except for a few with shallow groundwater source, slab-on-grade construction on very coarse soil. The above analysis shows that the greater weakness in prediction of α_{gw}^{in} may be in the prediction of α_{ss}^{in} . The value of 0.4 is a maximum for 95% of the cases examined, but the distribution extends to values as low as 10^{-5} (see Fig. 5). By comparison, the range of values for α_{ss}^{in} really does not extend to even two orders of magnitude (see Fig. 3).

It should be noted that the recommended α_{gw}^{in} as 0.004 is a bit more conservative than 0.001 suggested in the EPA's 2012 report [15]. The reason responsible for this might be that the screen of $c_{ss} > 500 \mu\text{g}/\text{m}^3$ is stricter compared to the source strength screens applied in the EPA's 2012 report [15]. Theoretically, independent of c_{gw} , low α_{gw}^{in} are more possible to be observed for subsets with low c_{ss} , but in the present study those subsets (with low c_{ss}) are excluded to generate a generic α_{gw}^{in} . In other words, the subsets screened in tend to have a higher α_{gw}^{in} . Nonetheless, these two values are still in the same order of magnitude.

4.4. Relationship between attenuation factor distributions and observed transients

The variations in all attenuation factors can in part be attributed to the differences in the particular physical situations, e.g., soil properties, contaminant source distribution, building construction features, but may also be associated with temporal variations during the assessments. Building operational parameters such as depressurization or air exchange rate can vary on the timescale of hours. In a recent paper by Holton et al. [40], a long-term and high-frequency sampling program was reported on the c_{in} in an individual house overlying a chlorinated solvent plume. During the two-year study, the TCE concentration in groundwater varied from 7 to $40 \mu\text{g}/\text{L}$, the air exchange rate fell in a range of 4–35 d^{-1} , and the c_{in} ranged from 0.01 to 20 ppbv (0.01 ppbv was the minimum detection limit). This range corresponds to 0.054 – $107 \mu\text{g}/\text{m}^3$. With reference to Fig. 4b, it may be seen that the lower of the values falls within the range that would be difficult to distinguish from normal background, but the higher values confirm that this structure is certainly influenced by VI. The c_{gw} calculated using Henry's law constant is in the range from 1920 to $11,000 \mu\text{g}/\text{m}^3$. A conservative estimate of c_{in} using the above 95% level source-to indoor attenuation factor of 0.004 is 7.7 – $44 \mu\text{g}/\text{m}^3$ (about 1.4–8.2 ppbv):

$$c_{in} = (1920 \sim 11,000) \mu\text{g}/\text{m}^3 \times 0.004 = (7.7 \sim 44) \mu\text{g}/\text{m}^3 \quad (12)$$

Both of these values are higher than 98% of the samples that would be taken at random times within the house [40], showing the conservatism of the 0.004 attenuation factor, even for prediction of such temporal variations. In that study, the temporal variation in VI was observed to be more significant in fall and winter seasons. The variation in A_e was measured to be no more than an order of magnitude over the entire test period, so the conclusion was drawn by the authors that it was necessarily variations in mass entry rate that were driving the temporal fluctuations. As already noted, the source concentration did not vary by an order of magnitude (and for the most part showed even lower variability). This does not permit definitively ascribing to either attenuation process (α_{ss}^{in} or α_{gw}^{in}) the majority of the temporal variation. On the one hand, depressurization might be greatest in heating seasons, resulting in greater mass entry rates at those times (and pointing to a role of α_{ss}^{in} variation). On the other hand, seasonal variability in soil moisture profiles could contribute to variations in α_{ss}^{in} . Given the two to three order of magnitude fluctuation in c_{in} , it is likely that several effects contribute.

The results of the Holton et al. [40] study also warn that the U.S. EPA's VI database likely contains similarly time-varying results. As a

result, it is unrealistic to look for very precisely defined attenuation factors from data sets that involve single measurements on many structures. There is likely to be an element of chance determining what concentrations are found at any particular site on any given day, a point that Holton et al. [40] illustrate well in their paper. The interesting question is the extent to which temporal concentration variability influences the observed variability in reported attenuation factors. The influence is quite likely already present in the data that have been used to obtain attenuation factors.

5. Conclusion

In this study, we re-examine the use of subsurface concentration as a criterion for determining the possible influence of subsurface sources on indoor air quality, and conclude that below a certain critical value as $500 \mu\text{g}/\text{m}^3$, it is unlikely that the source of low level indoor air contamination can be definitively attributed to vapor intrusion sources. This finding, in turn, permitted re-evaluation of the recommended “conservative” values of $\alpha_{\text{gw}}^{\text{in}}$ and $\alpha_{\text{ss}}^{\text{in}}$, which are found to be 0.004 and 0.02, respectively. The former is consistent with a controlled field study without influences of background sources. Ultimately, this study should help more confidently to identify buildings under the threat of VI, and offers a conservative overall source-to-indoor attenuation factor that is not very different from earlier empirical values suggested by U.S. EPA [15], but which is now more physically grounded in the different resistances characterizing source-to-slab and slab-to-indoor air processes.

Acknowledgements

This work was funded in the part by National Natural Science Foundation of China (No. 21307108 and No. 21177112), National Institute of Environmental Health Sciences (No. P42ES013660), National Basic Research Program of China (No. 2009CB421603), National Basic Research Program of China (No. Y201326597) and the Fundamental Research Funds for the Central Universities (No. 2014QNA6010).

References

- [1] U.S. EPA Office of Solid Waste and Emergency Response (OSWER), Draft of the Guidance for Evaluating the Vapor Intrusion to Indoor Air Pathway from Groundwater Soils (Subsurface Vapor Intrusion Guidance), OSWER, 2002 <http://www.epa.gov/osw/hazard/correctiveaction/eis/vapor/complete.pdf>
- [2] P.C. Johnson, R.A. Ettinger, Heuristic model for predicting the intrusion rate of contaminant vapors into buildings, *Environ. Sci. Technol.* 25 (8) (1991) 1445–1452.
- [3] U.S. EPA Office of Solid Waste and Emergency Response (OSWER), U.S. EPA's Vapor Intrusion Database, OSWER, 2002 http://www.epa.gov/oswer/vaporintrusion/vi_data.html
- [4] U.S. EPA Office of Solid Waste and Emergency Response (OSWER), Johnson and Ettinger (1991) Model for Subsurface Vapor Intrusion into Buildings, OSWER, 2002 http://www.epa.gov/oswer/riskassessment/airmodel/johnson_ettinger.htm
- [5] J.E. Johnston, J. Mac Donald Gibson, Probabilistic approach to estimating indoor air concentrations of chlorinated volatile organic compounds from contaminated groundwater: a case study in San Antonio, Texas, *Environ. Sci. Technol.* 45 (2011) 1007–1013.
- [6] J.E. Johnston, Q. Sun, J. Mac Donald Gibson, Updating exposure models of indoor air pollution due to vapor intrusion: Bayesian calibration of the Johnson–Ettinger model, *Environ. Sci. Technol.* 48 (2014) 2130–2138.
- [7] L. Zeng, L. Shi, D. Zhang, L. Wu, A sparse grid based Bayesian method for contaminant source identification, *Adv. Water Resources* 37 (2012) 1–9.
- [8] L. Shi, L. Zeng, J. Yang, D. Zhang, Multiscale-finite-element-based ensemble Kalman filter for large-scale groundwater flow, *J. Hydrol.* 468 (2012) 22–34.
- [9] L. Zeng, D. Zhang, A stochastic collocation based Kalman filter for data assimilation, *Comput. Geosci.* 14 (2010) 721–744.
- [10] Y. Yao, R. Shen, K.G. Pennell, E.M. Suuberg, A comparison of the Johnson–Ettinger vapor intrusion screening model predictions with full three-dimensional model results, *Environ. Sci. Technol.* 45 (12) (2011) 2227–2235.
- [11] Y. Yao, R. Shen, K.G. Pennell, E.M. Suuberg, A review of vapor intrusion models, *Environ. Sci. Technol.* 47 (2013) 2457–2470.
- [12] U.S. EPA Office of Solid Waste and Emergency Response (OSWER), Background Indoor Air Concentrations of Volatile Organic Compounds in North American Residences (1990–2005): A Compilation of Statistics for Assessing Vapor Intrusion, OSWER, 2011 <http://www.epa.gov/oswer/vaporintrusion/documents/oswer-vapor-intrusion-background-Report-062411.pdf>
- [13] T.E. McHugh, J.A. Connor, F. Ahmad, An empirical analysis of the groundwater-to-indoor-air exposure pathway: the role of background concentrations in indoor air, *Environ. Forensics* 5 (2004) 33–44.
- [14] J.E. Johnston, J. Mac Donald Gibson, Screening houses for vapor intrusion risks: a multiple regression analysis approach, *Environ. Sci. Technol.* 47 (2013) 5595–5602.
- [15] U.S. EPA Office of Solid Waste and Emergency Response (OSWER), EPA's Vapor Intrusion Database: Evaluation and Characterization of Attenuation Factors for Chlorinated Volatile Organic Compounds and Residential Buildings, OSWER, 2012 <http://www.epa.gov/oswer/vaporintrusion/documents/OSWER.2010.Database.Report.03-16-2012.Final.pdf>
- [16] Y. Yao, R. Shen, K.G. Pennell, E.M. Suuberg, Examination of the U.S. EPA's vapor intrusion database based on models, *Environ. Sci. Technol.* 47 (3) (2013) 1425–1433.
- [17] L.D.V. Abreu, P.C. Johnson, Effect of vapor source-building separation and building construction on soil vapor intrusion as studied with a three-dimensional numerical model, *Environ. Sci. Technol.* 39 (12) (2005) 4550–4561.
- [18] T.E. McHugh, L. Beckley, D. Bailey, K. Gorder, E. Dettenmaier, I. Rivera-Duarte, S. Brock, I.C. MacGregor, Evaluation of vapor intrusion using controlled building pressure, *Environ. Sci. Technol.* 46 (2012) 4792–4799.
- [19] Y. Yao, K.G. Pennell, E.M. Suuberg, Estimation of contaminant subsurface concentration in vapor intrusion, *J. Hazard. Mater.* 231–232 (2012) 10–17.
- [20] China Environmental Remediation, <http://www.chinaremmediation.com/news.20120823.2%20html>
- [21] S.S. Zhou, K.D. Lin, H.Y. Yang, L. Li, W. Liu, J. Li, Stereoisomeric separation and toxicity of a new organophosphorus insecticide chloramidophos, *Chem. Res. Toxicol.* 20 (3) (2007) 400–405.
- [22] C. Xu, M.R. Zhao, W.P. Liu, S.W. Chen, J.Y. Gan, Enantioselectivity in zebrafish embryo toxicity of the insecticide acetofenat, *Chem. Res. Toxicol.* 21 (5) (2008) 1050–1055.
- [23] C. Xu, J.J. Wang, W.P. Liu, G.Y. Sheng, Y.J. Tu, Y. Ma, Separation and aquatic toxicity of enantiomers of the pyrethroid insecticide lambda-cyhalothrin, *Environ. Toxicol. Chem.* 27 (1) (2008) 182–187.
- [24] U.S. EPA Office of Solid Waste and Emergency Response (OSWER), Conceptual Model Scenarios for the Vapor Intrusion Pathway, OSWER, 2012, February.
- [25] W.W. Nazaroff, Predicting the rate of ^{222}Rn entry from soil into basement of a dwelling due to pressure-driven air flow, *Radiat. Prot. Dosim.* 24 (1988) 199–202.
- [26] K.G. Pennell, M.K. Scammell, M.D. McClean, J. Ames, B. Weldon, L. Friguglietti, E.M. Suuberg, R. Shen, P.A. Indeglia, W.J. Heiger-Bernays, Sewer gas: an indoor air source of PCE to consider during vapor intrusion investigations, *Ground Water Monit. Rem.* 33 (3) (2013) 119–126.
- [27] H.E. Dawson, T. McAlary, A compilation of statistics for VOCs from post-1990 indoor air concentration studies in North American residences unaffected by subsurface vapor intrusion, *Ground Water Monit. Rem.* 29 (1) (2009) 60–69.
- [28] Massachusetts Department of Environmental Protection (MassDEP), Residential Typical Indoor Air Concentrations: Updates: Indoor Air Background, MCP Numerical Standard Documentation, MassDEP, 1992, et seq, as a Reference of Indoor Air Chemical Concentrations for Use in Evaluating a Potential Vapor Intrusion Pathway, MassDEP, 2008 <http://www.mass.gov/eea/docs/dep/cleanup/laws/jiatur.pdf>
- [29] New York State Department of Health (NYDOH), Final NYSDOH CEH BEEI Soil Vapor Intrusion Guidance: Appendix C Volatile Organic Chemicals in Air–Summary of Background Databases, NYDOH, 2006 http://www.health.ny.gov/environmental/investigations/soil_gas/svi_guidance/docs/svi_appendc.pdf
- [30] U.S. EPA. Building Assessment Survey and Evaluation (BASE) Study. 2001. <http://www.epa.gov/iaq/base/>
- [31] C.P. Weisel, J. Zhang, B.J. Turpin, M.T. Morandi, S. Colome, T.H. Stock, D.M. Spector, et al., Relationships of Indoor, Outdoor, and Personal Air (RIOPA), Health Effects Institute and National Urban Air Toxics Research Center, Boston, MA, and Houston, TX, 2015.
- [32] R. He, A. Ruan, C. Jiang, D. Shen, Responses of oxidation rate and microbial communities to methane in simulated landfill cover soil microcosms, *Bioresour. Technol.* 9 (2008) 7192–7199.
- [33] J. Wang, F.-F. Xia, Y. Bai, C.-R. Fang, Methane oxidation in landfill waste biocover soil: kinetics and sensitivity to ambient conditions, *Waste Manage.* 31 (2011) 864–870.
- [34] T.E. McHugh, L. Beckley, D. Bailey, K. Gorder, E. Dettenmaier, I. Rivera-Duarte, S. Brock, I.C. MacGregor, Evaluation of vapor intrusion using controlled building pressure, *Environ. Sci. Technol.* 46 (2012) 4792–4799.
- [35] Y. Yao, R. Shen, K.G. Pennell, E.M. Suuberg, Examination of the influence of environmental factors on contaminant vapor concentration attenuation factors using the U.S. EPA's vapor intrusion database, *Environ. Sci. Technol.* 47 (2) (2013) 906–913.

- [36] R. Shen, K.G. Pennell, E.M. Suuberg, Influence of soil moisture on soil gas vapor concentration for vapor intrusion, *Environ. Eng. Sci.* 30 (10) (2013) 628–637.
- [37] R. Shen, Y. Yao, K.G. Pennell, E.M. Suuberg, Modeling quantification of the influence of soil moisture on subsurface vapor concentration, *Environ. Sci.: Processes Impacts* 15 (2013) 1444–1451.
- [38] P.S. Lowell, B. Eklund, VOC emission fluxes as a function of lateral distance from the source, *Environ. Progress* 23 (1) (2004) 52–58.
- [39] Y. Yao, R. Shen, K.G. Pennell, E.M. Suuberg, Estimation of contaminant subsurface concentration in vapor intrusion including lateral source–building separation, *Vadose Zone J.* 12 (3) (2013), <http://dx.doi.org/10.2136/vzj2012.0157>.
- [40] C. Holton, H. Luo, P. Dahlen, K. Gorder, E. Dettenmaier, P.C. Johnson, Temporal variability of indoor air concentrations under natural conditions in a house overlying a dilute chlorinated solvent groundwater plume, *Environ. Sci. Technol.* 47 (2013) 13347–13354.